Properties of the Baranger Thawed Gaussian Propagator†

M. S. Child,* P. Sherratt, and Y. K. Sturdy

Oxford University, Physical and Theoretical Chemistry Laboratory, South Parks Road, Oxford OX1 3QZ, U.K.

Received: March 10, 2004; In Final Form: May 19, 2004

Properties of a new thawed Gaussian propagator, recently suggested by Baranger et al. for motion under a smoothed or averaged Hamiltonian, are examined for scaled Morse and quartic oscillators. The resulting power spectra are similar to those determined by Heller's thawed Gaussian wavepackets governed by the classical Hamiltonian, but markedly less accurate than the power spectra obtained by Herman−Kluk propagation. A phase modification to the new propagator implies a new semiclassical quantization formula, which is shown to be analytically equivalent to the Bohr−Sommerfeld form for the Morse oscillator, for parameter values appropriate to molecular systems. Small differences between the two forms for the quartic oscillator are found to depend on the width of the coherent state used for the smoothing.

1. Introduction

A number of recent publications have raised the connection between thawed Gaussian wavepackets and Herman−Kluk dynamics. In particular, Baranger et al.[1] gave a very careful path integral derivation of the thawed Gaussian wavepacket moving over a smoothed, or ordered, Hamiltonian, $H_{ord}(z^*, z)$, averaged over a continuous set of frozen Gaussian functions, or coherent states $|z\rangle = |p, q\rangle$. The resulting form differs from that given, for example by Kay[2] for motion over the classical Hamiltonian, by the inclusion of an additional phase term, both derivations being subject to the approximation that the appropriate Hamiltonian is expanded to quadratic terms about a guiding reference trajectory. Following an approach initiated by Miller,[3] Child and Shalashilin[4] showed that the matrix element of the Herman−Kluk propagator, evaluated in the same quadratic approximation to the averaged Hamiltonian, was in effect identical with a projection of the Baranger thawed Gaussian form onto a final coherent state $|z_f\rangle$, although the connection with Baranger et al.[1] was not made explicit. Discussion has arisen[6−8] from the claim that the Baranger thawed Gaussian form, or mixed propagator, was more logically derived and more accurate than the Herman−Kluk propagator, a view that was challenged by Grossman and Herman[6] and later somewhat modified.[8] The present paper addresses a different aspect of the discussion, by using the power spectra derived by the two thawed Gaussian propagation schemes (classical and averaged) to examine connections between the Bohr−Sommerfeld quantization formula for motion on the classical Hamiltonian, with a modified formula for motion under the averaged one, of which the latter is a slight variant of a form suggested by Baranger et al.[1] Second, we compare the results with those obtained by Herman−Kluk propagation and by Bohr−Sommerfeld quantization.

Two systems are chosen for investigation: the Morse oscillator and a pure quartic oscillator. The Morse oscillator is particularly simple because the dynamics under both the Hamiltonian forms can be treated analytically. Moreover, Bohr−Sommerfeld quantization is exact. The quartic oscillator is interesting for the opposite reason that Bohr−Sommerfeld quantization is notoriously inaccurate for the lowest states.[10]

The organization of the paper is straightforward. Quantization is achieved, in the usual way, by Fourier transformation of the autocorrelation function. The necessary working equations for the thawed Gaussian wavepackets are given in section 2, together with the phase integral quantization formulas. Applications to the Morse and quartic oscillator systems are given in sections 3 and 4, respectively. Section 5 summarizes the overall conclusions. Finally, analytical properties of the Morse oscillator, including new formulas for the monodromy matrix elements, are given in the appendix.

2. Thawed Gaussian Auto Correlation Functions and Power Spectra

We follow Baranger et al.[1] in using the Klauder[13] phase convention for the coherent states, in which case the mixed propagator for motion under the averaged Hamiltonian, given by eq 4.29 of Baranger,[1] may be expressed as

$$\langle x|e^{-iH_{av}t/\hbar}|p_0, q_0\rangle = N\exp\left\{-\frac{\gamma_t}{2}[x-q_{it}]^2+\frac{i}{\hbar}p_{it}[x-q_{it}]+\frac{i}{\hbar}\left[S_{av}+T+\frac{1}{2}p_0q_0\right]\right\} \quad (1)$$

where the normalization factor, N, and the thawed exponent, γ_t, may be represented in terms of monodromy matrix elements[2] in the forms

$$N=\left(\frac{\gamma_0}{\pi}\right)^{1/4}(M_{qq}+i\hbar\gamma_0M_{qp})^{-1/2}$$

and

$$\gamma_t=\gamma_0\left(\frac{M_{pp}-\frac{i}{\hbar\gamma_0}M_{pq}}{M_{qq}+i\hbar\gamma_0M_{qp}}\right) \quad (2)$$

Other notations in eq 1 include

$$S_{av}=\int_0^t[p_i\dot{q}_i-H_{av}(p_i, q_i)]\,dt \quad (3)$$

$$H_{av}=\frac{1}{2m}p^2+V_{av}+\frac{\gamma_0\hbar^2}{4m} \quad (4)$$

† Part of the "Gert D. Billing Memorial Issue".

10.1021/jp040208x CCC: $27.50
Published on Web 07/16/2004

and

$$T = \frac{1}{4}\int_0^t \left(\frac{1}{\gamma_0} \frac{\partial^2 V_{\mathrm{av}}}{\partial q^2} + \frac{\gamma_0 \hbar^2}{m} \right) \mathrm{d}t \tag{5}$$

where the term $\gamma_0\hbar^2/m$ arises from the kinetic energy part of H_{av}. Equation 1 differs from the equivalent form for motion under the classical Hamiltonian[2,11] by the fact that the trajectories and the action S_{cl} are governed by H_{av}, and that the term T is absent from the classical form. It is also readily shown, in the case of a globally quadratic Hamiltonian, that H_{av} differs from H_{cl} by a constant "local zero-point energy" such that $S_{\mathrm{av}} + T$ is precisely equal to S_{cl}.[4]

The next step is to calculate the appropriate autocorrelation function. Following Child and Shalashilin,[4] the appropriate form for the Baranger case of motion under H_{av} is given by

$$C_{\mathrm{av}}(t) = \langle p_0, q_0 | e^{-iH_{\mathrm{av}}t/\hbar} | p_0, q_0 \rangle = \frac{\langle p_0, q_0 | p_t, q_t \rangle}{\sqrt{M_{z^*z^*}}} \times \exp\left\{ \frac{1}{2} M_{zz^*} (M_{z^*z^*})^{-1} (z_0^* - z_t^*)^2 + \frac{i}{\hbar}(S_{\mathrm{av}} + T) \right\} \tag{6}$$

where

$$M_{zz^*} = \frac{1}{2}\left(M_{qq} - M_{pp} + i\hbar\gamma_0 M_{qp} + \frac{i}{\hbar\gamma_0} M_{pq} \right) \tag{7}$$

$$M_{z^*z^*} = \frac{1}{2}\left(M_{qq} + M_{pp} + i\hbar\gamma_0 M_{qp} - \frac{i}{\hbar\gamma_0} M_{pq} \right) \tag{8}$$

$$\langle p_0, q_0 | p_t, q_t \rangle = \exp\left\{ -\frac{\gamma_0}{4}(q_t - q_0)^2 - \frac{1}{4\gamma_0\hbar^2}(p_t - p_0)^2 + \frac{i}{\hbar}(p_t + p_0)(q_t - q_0) \right\} \tag{9}$$

and

$$z_0^* = \sqrt{\frac{\gamma_0}{2}}\left(q_0 - \frac{i}{\gamma_0\hbar} p_0 \right) \tag{10}$$

with an equivalent form for z_t^*. The appropriate form for motion under the classical Hamiltonian is obtained by substituting S_{cl} for $S_{\mathrm{av}} + T$.

The corresponding form for the Herman−Kluk autocorrelation function appears as an integral over initial phase points (p_i, q_i)

$$C_{\mathrm{HK}}(t) = \int\int \langle p_0, q_0 | p_{it}, q_{it} \rangle \sqrt{M_{z_i z_i}}\, e^{iS_{cl}/\hbar} \langle p_{i0}, q_{i0} | p_0, q_0 \rangle \frac{dp_{i0} dq_{i0}}{2\pi\hbar} \tag{11}$$

in which $M_{z_i z_i}$ is the complex conjugate of the form in eq 8, evaluated for the ith trajectory.

Finally, the power spectra are given by

$$P(E) = \frac{1}{\pi} Re \int_0^{t_{\max}} C(t) e^{i(E + i\alpha)t/\hbar}\, \mathrm{d}t \tag{12}$$

where the exponent α is chosen to reduce the integrand to a negligible value at $t = t_{\max}$. Peaks occur at energy values such that contributions from successive cycles of the classical motion combine in phase. Hence an analysis of the origin of such peaks may be used to provide a semiclassical quantization condition for motion under H_{av}. Bearing in mind that the pre-exponent term, $(M_{z^*z^*})^{-1/2}$, in eq 6 contributes a phase factor of $e^{-i\pi}$ for each cycle, with period τ, the condition for constructive interference in the averaged case may be expressed as

$$\frac{1}{2\pi\hbar}[S_{\mathrm{av}}(\tau) + T(\tau) + E\tau] - \frac{1}{2} = \upsilon \tag{13}$$

because the remaining terms in eq 6 come back to themselves after each cycle.

The connection with the Bohr−Sommerfeld formula for quantization of the classical Hamiltonian,

$$I = \frac{1}{2\pi}\int_0^\tau p\dot{q}\, \mathrm{d}t = \left(\upsilon + \frac{1}{2} \right)\hbar \tag{14}$$

may be established by rewriting eq 13 as

$$\frac{1}{2\pi}\int_0^\tau \left[p\dot{q} + \frac{1}{4\gamma_0}\frac{\partial^2 V_{\mathrm{av}}}{\partial q^2} + \frac{\gamma_0\hbar^2}{4m} - H_{\mathrm{av}} + E \right] \mathrm{d}t = \left(\upsilon + \frac{1}{2} \right)\hbar \tag{15}$$

Hence the analogue of eq 14 is conveniently written as

$$\frac{1}{2\pi}\int_0^\tau \left[p\dot{q} + \frac{1}{4\gamma_0}\frac{\partial^2 V_{\mathrm{av}}}{\partial q^2} \right] \mathrm{d}t = \left(\upsilon + \frac{1}{2} \right)\hbar \tag{16}$$

with the energy of the trajectory chosen such that

$$E = H_{\mathrm{av}} - \frac{\gamma_0\hbar^2}{4m} = \frac{1}{2m}p^2 + V_{\mathrm{av}} \tag{17}$$

because the term $\gamma_0\hbar^2/4m$ from the T integral in eq 4 cancels with an identical contribution to H_{av}. A less heuristic derivation of eq 16, without this cancellation, is given by Baranger et al.[1] (see eq 6.62).

3. Morse Oscillator

Classical and Averaged Hamiltonians. It may be verified by scaling the energy, coordinate, and momentum and energy by α, $\hbar/\alpha$ and $\hbar^2/2m$, with $\alpha = (\hbar^2 2ma^2 D)^{1/4}$, that the classical Hamiltonian reduces to the scaled form

$$H_{\mathrm{cl}} = \frac{1}{2}p_x^2 + D(1 - e^{-ax})^2 \quad a = 1/\sqrt{2D} \tag{18}$$

with $\hbar = 1$. In addition it turns out, by averaging the quantum analogue of H_{cl} over the coherent state $|pq\rangle$, with exponent γ_0, that the averaged Hamiltonian also takes the Morse form

$$H_{\mathrm{av}} = H_0 + \frac{1}{2}p^2 + D'(1 - e^{-aq'})^2 \tag{19}$$

where

$$H_0 = \gamma_0/4 + D - D',\ D' = De^{-a^2/2\gamma_0} \quad q' = q - 3a/4\gamma_0 \tag{20}$$

In addition, the integrand in eq 8 is given by

$$\frac{1}{4}\left(\frac{1}{\gamma_0}\frac{\partial^2 H_{\mathrm{av}}}{\partial q^2} + \gamma_0\hbar^2 \frac{\partial^2 H_{\mathrm{av}}}{\partial p^2} \right) = \frac{\gamma_0}{4} + \frac{a^2 D'}{2\gamma_0}(2e^{-2aq'} - e^{-aq'}) \tag{21}$$

All the quantities required for evaluation of the two thawed Gaussian autocorrelation functions, including new expressions for the monodromy matrix elements, may be evaluated with

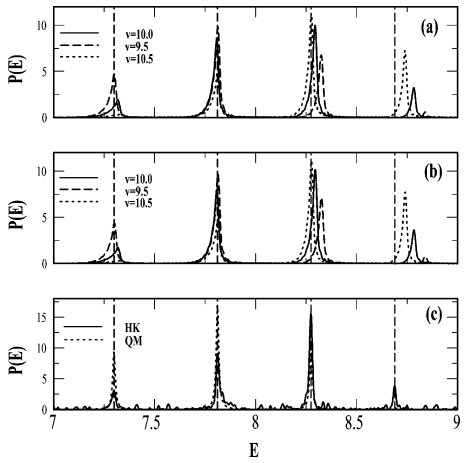

Figure 1. Morse oscillator power spectra obtained by (a) the classical thawed Gaussian approximation (TGA), (b) the averaged TGA, and (c) Herman−Kluk propagation.

the help of the angle-action expressions listed in the appendix. We first compare the forms of the resulting power spectra, with the power spectrum obtained by Herman−Kluk propagation and then compare the quantization formulas (eqs 14 and 16).

Power Spectra. Figures 1a−c show the "classical", "averaged" and Herman−Kluk power spectra, respectively, for a scaled Morse oscillator with $D = 10.25$, for which the quantum energies are indicated by vertical dashed lines. In each case the initial coherent state $|p_0, q_0\rangle$, with width parameter $\gamma_0 = 1$, was centered at the right-hand turning point for the appropriate motion. The autocorrelation functions were propagated for 25 cycles of the classical motion, and damped with an exponent $\alpha = \log(300)/T$ in eq 12. The three spectra illustrated in Figures 1a and 1b were obtained for classical actions $I = (\upsilon + 1/2)$, with $\upsilon = 9.5$, 10, and 10.5. The corresponding energy in eq 17, for the "averaged" case, was taken as the classical energy given by eq 22 below. The Herman−Kluk autocorrelation function in eq 11 was approximated by Monte Carlo quadrature over 500 trajectories; results were independent of the precise location of $|p_0, q_0\rangle$.

It is of course no surprise that the Herman−Kluk spectrum is superior to the two thawed Gaussian spectra. This superiority of a frozen multi-Gaussian propagator was demonstrated by Kay[2] 10 years ago, and even the multitrajectory variant of thawed Gaussian propagation was recently shown[9] to be inferior to the HK approach. It is interesting for what follows to see almost precise equivalence, in the present Morse oscillator case, with the true quantum mechanical spectrum (shown by dots), obtained by Lorentzian convolution of $|\langle\psi_\upsilon||p_0, q_0\rangle|^2$ with a width parameter α. It is also seen that the "classical" and "averaged" thawed Gaussian spectra are virtually identical, each with one well-reproduced peak at the energy of the 10th eigenstate ($E \simeq 7.8$) but with progressively large discrepancies for the other peaks, depending on the precise starting conditions. The origin of these discrepancies is simply that the autocorrelation function of any single thawed Gaussian wavepacket is necessarily modulated by the period of the classical motion, which is reflected in the power spectrum by a pattern of equally spaced peaks, with a separation dictated by the classical frequency. By contrast the potential anharmonicity is properly taken into account, in the Herman−Kluk method, by decomposing the initial wavepacket into a swarm of coherent states, each with its own characteristic frequency. Note, however, that the presence of the spurious peaks in Figures 1a and 1b goes some way to explaining the size of the required HK swarm. The large swarm is not simply required as a crude root search for trajectories at the eigen-energies. It is also required to eliminate the spurious sideband peaks, by destructive interference.

Semiclassical Quantization. To understand the features of the thawed Gaussian spectra in more detail, it is simplest first to consider the "classical" case, for which the Hamiltonian takes the angle-action form

$$H_{\rm cl} = I - \frac{I^2}{4D} \tag{22}$$

with the period of the trajectory given by $\tau = 2\pi/\omega$, where

$$\omega = \frac{\partial H_{\rm cl}}{\partial I} = 1 - \frac{I}{2D} \tag{23}$$

The "classical" analogue of eq 15 therefore rearranges to

$$\frac{1}{2\pi}\int_0^\tau [p\dot{q} - H_{\rm cl} + E]\,{\rm d}t = \left(I - \frac{[H_{\rm cl} - E]}{\omega}\right) = \upsilon + \frac{1}{2} \tag{24}$$

where υ is an integer. Written in another way, with $I = \upsilon + 1/2 + \delta$

$$E = \left(\upsilon + \frac{1}{2}\right)\left(1 - \frac{I}{2D}\right) + \frac{I^2}{4D} = \upsilon + \frac{1}{2} - \frac{\left(\upsilon + \frac{1}{2}\right)^2}{4D} + \frac{\delta^2}{4D} \tag{25}$$

In other words, as seen in Figure 1a, the "classical" thawed Gaussian power spectrum, based on a trajectory with action $I = \upsilon + 1/2$, precisely reproduces the υth eigenvalue, but all other eigenvalues have errors proportional to $(\upsilon + 1/2 - I)^2$.

Turning to the connection between the "classical" and "averaged" spectra in Figures 1a and 1b, note first that the actions, I for the classical and I' for the averaged motion, may be related by using eq A.2 in the appendix to express eqs 17 and 19 in angle action form. One finds, on equating the resulting energy expression with $H_{\rm cl}$ in eq 22, that

$$E = I - \frac{I^2}{4D} = \sqrt{\frac{D'}{D}}I' - \frac{I'}{4D} + D - D' \tag{26}$$

which rearranges to

$$I = I' + 2(D - \sqrt{DD'}) \tag{27}$$

Second, the angle-action identity (eq A.3)

$$e^{-aq'} = \frac{1 - \epsilon'}{1 + \sqrt{\epsilon'}\cos\theta} \qquad \epsilon' = \frac{E - (D - D')}{D'} \tag{28}$$

may be verified to yield

$$\frac{1}{8\pi\gamma_0}\int_0^\tau \frac{\partial^2 V_{\rm av}}{\partial q^2}\,{\rm d}t = \frac{a^2 D'}{8\pi\gamma_0\omega'}\int_0^{2\pi}(2e^{-2aq'} - e^{-aq'})\,{\rm d}\theta = 2\sqrt{DD'}\frac{a^2}{4\gamma_0} \tag{29}$$

after noting that $\omega' = \partial H_{\rm av}/\partial I' = \sqrt{(1-\epsilon')D'/D}$. Consequently, within the approximation

$$\frac{a^2}{4\gamma_0} \simeq e^{a^2/4\gamma_0} - 1 = \sqrt{\frac{D}{D'}} - 1 \tag{30}$$

equation 16 goes over to

$$\frac{1}{2\pi}\int_0^\tau \left[p\dot{q} + \frac{1}{4\gamma_0}\frac{\partial^2 V_{\mathrm{av}}}{\partial q^2}\right] \mathrm{d}t = I' + 2(D - \sqrt{DD'}) = \left(v + \frac{1}{2}\right)\hbar \tag{31}$$

Taken in conjunction with eq 27, this means that the modified quantization formula for the averaged Hamiltonian reduces to the classical Bohr−Sommerfeld expression, within the validity of eq 30. This underlying identity explains the close similarity between Figures 1a and 1b, which is likely to apply in all practical molecular situations, with $N > 10$, because with the present scaling, $N = 2D = 1/a^2$, while it is natural to choose γ_0 close to unity, to minimize H_0. Consequently the exponent in eq 30 is of the order $a^2/4\gamma_0 \simeq (4N)^{-1} \ll 1$.

4. Quartic Oscillator

Classical and Averaged Hamiltonians. The scaled quartic oscillator Hamiltonian is taken in the form

$$H_{\mathrm{cl}} = \frac{1}{2}p^2 + \frac{1}{2}q^4 \tag{32}$$

with $\hbar = 1$, in which case the averaged counterpart becomes

$$H_{\mathrm{av}} = \frac{1}{2}p^2 + \frac{3}{2\gamma_0}q^2 + \frac{1}{2}q^4 + \frac{\gamma_0}{4} + \frac{3}{8\gamma_0^2} \tag{33}$$

so that

$$\frac{1}{4\gamma_0}\frac{\partial^2 V_{\mathrm{av}}}{\partial q^2} = \frac{3}{4\gamma_0^2} + \frac{3}{2\gamma_0}q^2 \tag{34}$$

Power Spectra. Figure 2 gives a similar comparison between the thawed Gaussian and Herman−Kluk power spectra to that shown in Figure 1; but the results are rather different. The coherent state exponent was taken as $\gamma_0 = 3^{1/3}$, which minimizes the constant part of H_{av}. The energy of the initial wavepacket was chosen as that of the $v = 1$ eigenstate ($E \simeq 1.9$). Each autocorrelation function was again propagated for 25 periods, using 500 Herman−Kluk trajectories.

Again, the two thawed Gaussian spectra in Figures 2a and 2b reproduce a single eigenvalue moderately well but the others very poorly. The subsidiary peaks in Figure 2a now lie below the eigenvalues, because the quartic oscillation frequency increases with energy, and the peak spacing in Figure 2b is even wider due to the added quadratic term in $V_{\mathrm{av}}(q)$. Another significant difference from the Morse oscillator case is that the Herman−Kluk propagator fails to reproduce the quartic oscillator eigenvalues. Instead, the peaks in Figure 2c closely coincide with the Bohr−Sommerfeld eigenvalues, in Table 1 below. The origin of this Bohr−Sommerfeld equivalence is addressed in the concluding section.

Semiclassical Quantization. Turning to the question of semiclassical quantization, the Bohr−Sommerfeld formula (eq 14) for the classical motion takes the form

$$v + \frac{1}{2} = \frac{1}{2\pi}\oint p\,\mathrm{d}q = \frac{2}{\pi}\int_0^{q_0} \sqrt{2E - q^4}\,\mathrm{d}q$$
$$= \frac{(2E)^{3/4}}{2\pi}\int_0^1 u^{-3/4}\sqrt{1-u}\,\mathrm{d}u = \frac{(2E)^{3/4}}{2\pi}\frac{\Gamma(1/4)\Gamma(3/2)}{\Gamma(7/4)} \tag{35}$$

where $q_0 = (2E)^{1/4}$. The corresponding integral (eq 16) for the averaged Hamiltonian case may be evaluated in terms of elliptic integrals.[15] The first step is to write eq 17 in the form

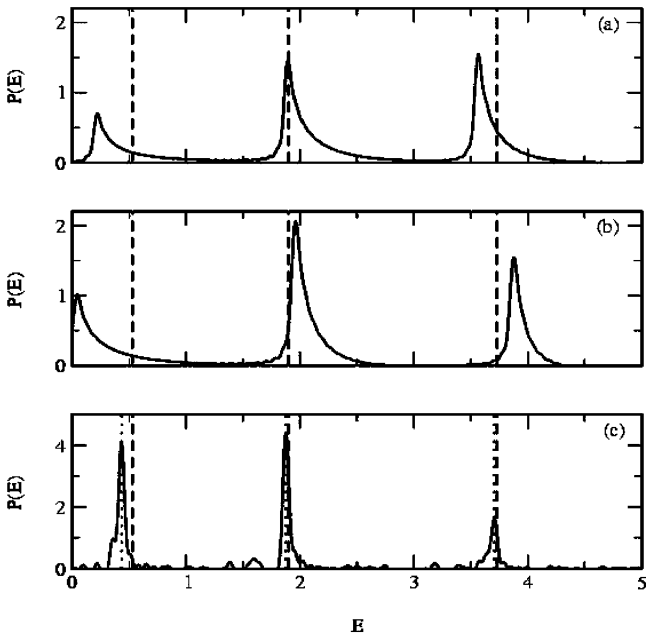

Figure 2. Quartic oscillator power spectra obtained by (a) "classical" TGA, (b) "averaged" TGA, and (c) HK propagation. The dashed verticals indicate the quantum mechanical eigenvalues. The dotted ones in panel (c) are Bohr−Sommerfeld eigenvalues.

TABLE 1: Comparison between Exact and Semiclassical Eigenvalues for the Quartic Hamiltonian[a]

v	exact	classical	averaged $\gamma_0 = 1$	averaged $\gamma_0 = 3^{1/3}$	averaged $\gamma_0 = 10$
0	0.53018	0.43351	0.46056	0.46480	0.43529
1	1.89984	1.87596	1.97545	1.93709	1.87776
2	3.72785	3.70699	3.83247	3.77719	3.70882
3	5.82238	5.80576	5.94469	5.88040	5.80760
4	8.130915	8.11680	8.26400	8.19412	8.11865
5	10.61919	10.60681	10.75964	10.68593	10.60867
10	25.12813	25.120045	25.28622	25.20338	25.12193

[a] The headings "classical" and "averaged" refer to quantization by eqs 34 and 38, respectively.

$$p^2 = 2[E - V_{\mathrm{av}}(q)] = 2E - q^4 - \frac{3q^2}{\gamma_0} - \frac{3}{4\gamma_0^2}$$
$$= (a_+^2 + q^2)(a_-^2 - q^2) \tag{36}$$

where

$$a_\pm^2 = \sqrt{2E + \frac{3}{2\gamma_0^2}} \pm \frac{3}{2\gamma_0} \tag{37}$$

Second, bearing in mind that $\dot{q} = p$ in the present units, eq 16 may be reexpressed as

$$\left(v + \frac{1}{2}\right) =$$
$$\frac{1}{2\pi}\int_0^\tau \left[p\dot{q} + \frac{V_{\mathrm{av}}''}{4\gamma_0}\frac{\dot{q}}{p}\right]\mathrm{d}t = \frac{2}{\pi}\int_0^{a_-} \frac{[p^2 + V_v''/4\gamma_0]}{\sqrt{(a_+^2 + q^2)(a_-^2 - q^2)}}\,\mathrm{d}q \tag{38}$$

Finally, the numerator can be expressed, with the help of eqs 34 and 36, in terms of tabulated integrals.[15] The final form becomes

$$v + \frac{1}{2} = \frac{1}{6\pi}\{(a_+^4 - a_-^4 + 8a_+^2 a_-^2)\,K(k) + 2(a_+^4 - a_-^4)\,E(k)\} \tag{39}$$

where $K(k)$ and $E(k)$ are elliptic integrals of the first and second types, with the argument

$$k^2 = \frac{a_-^2}{a_+^2 + a_-^2} \tag{40}$$

Table 1 gives a comparison between the exact eigenvalues and those given by eqs 35 and 39, including information on the sensitivity of the latter to the choice of γ_0. The special value $\gamma_0 = 3^{1/3}$ gives a minimum zero-point energy of 0.540844. It is noticeable that the "classical" and "averaged" semiclassical eigenvalues are seriously inaccurate for $v = 0$. Second, the $v = 1$ eigenvalues in columns 2 and 4 closely correspond to the positions of the central peaks in Figures 2a and 2b. Finally, the "averaged" eigenvalues values tend toward the "classical" ones as γ_0 increases.

5. Summary and Conclusions

Power spectra determined by thawed Gaussian propagation under the Hamiltonian, H_{cl}, in its classical form and in its coherent state averaged form, H_{av}, were compared with the spectrum obtained by Herman−Kluk propagation for the Morse oscillator and a quartic oscillator. The most important outcome of the analysis concerns the relationship between the modified quantization eqs 16−17 for motion under the "averaged" Hamiltonian and the Bohr−Sommerfeld quantization formula (eq 14) for normal "classical" motion. A remarkable feature of the Morse oscillator system is that the "classical" and "averaged" thawed Gaussian spectra in Figures 1a and 1b are indistinguishable on the scale of the diagram, a feature which is traced to analytical equivalence between the two quantization schemes, provided that the weak approximation (eq 30) is satisfied. A similar analysis, for the quartic oscillator, showed agreement between the two quantization schemes only in the limit $\gamma_0 \gg 1$. Both methods were seriously inaccurate for the lowest eigenvalue, with a slight advantage for the modified (averaged Hamiltonian) scheme, while the classical Bohr−Sommerfeld formula was more accurate for the higher eigenvalues.

A second significant conclusion is that, although the two types of thawed Gaussian wavepackets give a good approximation to the eigenvalue closest in energy to that of the guiding trajectory, the results are markedly inferior to those obtained by Herman−Kluk propagation, although the latter is shown, by the quartic oscillator example, to approximate the Bohr−Sommerfeld eigenvalues, rather than the exact ones. The weakness of any single trajectory thawed Gaussian approach is that the power spectrum inevitably contains sideband peaks, separated from the main peak by uniform intervals determined by the frequency of the guiding trajectory. By contrast, the Herman−Kluk spectra combine information from a swarm of trajectories in such a way that the spurious sideband peaks are removed by destructive interference to be replaced by peaks, which are shown by the quartic oscillator example, to coincide with the semiclassical Bohr−Sommerfeld eigenvalues, rather than the exact ones. We cannot at present give a proof of this equivalence, but it is easy to see, from the argument given above, that members of the swarm at the true quantum mechanical eigenvalues will produce spectral peaks at the correct positions because each HK term contributes the same classical action and turning point contribution as a classical thawed Gaussian at the same energy. It is, however, less easy to demonstrate that destructive interference will necessarily eliminate all the spurious sideband peaks.

Acknowledgment. The authors are grateful to Dr. D. V. Shalashilin for helpful discussions. P.S. acknowledges financial support from UK EPSRC.

Appendix A: Properties of the Morse Oscillator

Basic Equations. Analytical properties of the Morse oscillator, with the Hamiltonian

$$H = \frac{1}{2\mu}p^2 + D(1 - e^{-aq})^2 \tag{A.1}$$

are conveniently based on the angle-action forms collected by Child.[14] The corresponding action form is

$$H = \sqrt{\frac{2a^2D}{\mu}}I - \frac{a^2}{2\mu}I^2 \tag{A.2}$$

In addition, the coordinate $q(\theta)$ and momentum $p(\theta)$ vary with the angle variable θ as

$$q(\theta) = \frac{1}{a}\ln\left(\frac{1 + \sqrt{\epsilon}\cos\theta}{1 - \epsilon}\right)$$

and

$$p(\theta) = -\frac{\delta \sin\theta}{1 + \sqrt{\epsilon}\cos\theta} \tag{A.3}$$

where $\epsilon = E/D$, $\delta = \sqrt{2\mu D\epsilon(1-\epsilon)}$, and θ increases linearly with time, $\theta = \theta_0 + \omega t$, at a frequency

$$\omega = \frac{\partial H}{\partial I} = \sqrt{\frac{2a^2D}{\mu}}\left(1 - \sqrt{\frac{a^2}{2\mu D}}I\right) = \sqrt{\frac{2a^2D(1-\epsilon)}{\mu}} \tag{A.4}$$

Monodromy Matrix Elements. Analytical expressions for the monodromy matrix elements are also available, by noting that[2]

$$\begin{pmatrix} \dot{M}_{pp} & \dot{M}_{qp} \\ \dot{M}_{qp} & \dot{M}_{qq} \end{pmatrix} = \begin{pmatrix} 0 & -V'' \\ \mu^{-1} & 0 \end{pmatrix}\begin{pmatrix} M_{pp} & M_{pq} \\ M_{qp} & M_{qq} \end{pmatrix} \tag{A5}$$

with the boundary condition $M(0) = I$. Consequently, the elements M_{qr}, where $r = q$ or p, satisfy the same linear differential equation as the momentum, namely,

$$\frac{d^2M}{dt^2} = -\frac{V''(q)}{\mu}M \tag{A.6}$$

Since the angle θ increases linearly with time, it follows that the Wronskian of $p(\theta)$ with $M(\theta)$ is constant,

$$p(\theta)\frac{\mathrm{d}M}{\mathrm{d}\theta} - M(\theta)\frac{\mathrm{d}p}{\mathrm{d}\theta} = -A\delta = \text{const} \tag{A.7}$$

Consequently, by use of the integrating factor $p^{-1}(\theta)$,

$$\frac{M(\theta)}{p(\theta)} = -\frac{A}{\delta}\int\frac{\mathrm{d}\theta}{p^2(\theta)} + \frac{B}{\delta}$$

$$= -\frac{A}{\delta}\int\left[(1+\epsilon)\csc^2\theta + \frac{2\epsilon^{1/2}\cos\theta}{\sin^2\theta} - \epsilon\right]\mathrm{d}\theta + \frac{B}{\delta} \tag{A.8}$$

from which

$$M(\theta) = A\frac{(1+\epsilon)\cos\theta + 2\epsilon^{1/2} + \epsilon\theta\sin\theta}{1+\epsilon^{1/2}\cos\theta} + B\frac{\sin\theta}{1+\epsilon^{1/2}\cos\theta} \quad \text{(A.9)}$$

It is also evident, from eq A.5 that the elements M_{pr}, where $r = q$ or p, collectively denoted $N(\theta)$, are related to $M(\theta)$ by

$$N(\theta) = \mu\omega\frac{dM}{d\theta} \quad \text{(A.10)}$$

We now choose standard solutions of the $M(\theta)$ type, namely $f_{qq}(\theta)$ and $f_{qp}(\theta)$, and of the $N(\theta)$ type, namely $f_{pq}(\theta)$ and $f_{pp}(\theta)$, such that

$$\begin{pmatrix} f_{qq}(0) & f_{qp}(0) \\ f_{pq}(0) & f_{pp}(0) \end{pmatrix} = \begin{pmatrix} 1 & 0 \\ 0 & 1 \end{pmatrix} \quad \text{(A.11)}$$

The first column of eq A.11 is satisfied by the coefficient choice, $A = (1+\epsilon^{1/2})^{-1}$, $B = 0$ in eqs A.9−A.10), and the second by $A = 0$, $B = (1+\epsilon^{1/2})/\mu\omega$. The resulting functional forms are found to be

$$f_{qq}(\theta) = \frac{(1+\epsilon)\cos\theta + 2\epsilon^{1/2} + \epsilon\theta\sin\theta}{(1+\epsilon^{1/2})(1+\epsilon^{1/2}\cos\theta)} \quad \text{(A.12)}$$

$$f_{pq}(\theta) = \frac{\mu\omega}{(1+\epsilon^{1/2})}\left\{\frac{\epsilon\theta\cos\theta - \sin\theta}{(1+\epsilon^{1/2}\cos\theta)} + \frac{\epsilon^{1/2}\sin\theta[(1+\epsilon)\cos\theta + 2\epsilon^{1/2} + \epsilon\theta\sin\theta]}{(1+\epsilon^{1/2}\cos\theta)^2}\right\} \quad \text{(A.13)}$$

$$f_{qp}(\theta) = \frac{(1+\epsilon^{1/2})\sin\theta}{\mu\omega(1+\epsilon^{1/2}\cos\theta)} \quad \text{(A.14)}$$

$$f_{pp}(\theta) = \frac{(1+\epsilon^{1/2})(\epsilon^{1/2}+\cos\theta)}{(1+\epsilon^{1/2}\cos\theta)^2} \quad \text{(A.15)}$$

Equations A.12−A.15 give the monodromy matrix elements for propagation from $\theta = 0$ at energy $E = \epsilon D$. The forms for propagation from other different initial angles θ_0 are given by

$$M_{qq}(\theta) = f_{pp}(\theta_0)f_{qq}(\theta) - f_{pq}(\theta_0)f_{qp}(\theta) \quad \text{(A.16)}$$

$$M_{pq}(\theta) = f_{pp}(\theta_0)f_{pq}(\theta) - f_{pq}(\theta_0)f_{pp}(\theta) \quad \text{(A.17)}$$

$$M_{qp}(\theta) = f_{qq}(\theta_0)f_{qp}(\theta) - f_{qp}(\theta_0)f_{qq}(\theta) \quad \text{(A.18)}$$

$$M_{pp}(\theta) = f_{qq}(\theta_0)f_{pp}(\theta) - f_{qp}(\theta_0)f_{pq}(\theta) \quad \text{(A.19)}$$

References and Notes

(1) Baranger, M.; de Aguiar, M. A. M.; Keck, F.; Korsch, H. J.; Schellhaass, B. *J. Phys. A* **2001**, *34*, 7227.

(2) Kay, K. G. *J. Chem. Phys.* **1994**, *100*, 4377

(3) Miller, W. H. *J. Phys. Chem. B* **2002**, *106*, 8132.

(4) Child, M. S.; Shalashilin, D. V. *J. Chem. Phys.* **2003**, *118*, 2061.

(5) Herman, M. F.; Kluk, E. *Chem Phys.* **1984**, *85*, 2069.

(6) Grossmann, F.; Herman, M. F. *J. Phys. A* **2002**, *35*, 9489.

(7) Baranger, M.; de Aguiar, M. A. M.; Keck, F.; Korsch, H. J.; Schellhaass, B. *J. Phys. A* **2002**, *35*, 9493.

(8) Baranger, M.; de Aguiar, M. A. M.; Korsch, H. J. *J. Phys. A* **2002**, *35*, 9795.

(9) Harabati, C.; Rost, J. M.; Grossman, F. *J. Chem. Phys.* **2004**, *120*, 26.

(10) Balian, R.; Parisi, G.; Voros, A. *Phys. Rev. Lett.* **1978**, *41*, 1141.

(11) Heller, E. J. *J. Chem. Phys.* **1975**, *62*, 1544.

(12) Ehrenfest, P. *Zeit. Phys.* **1927**, *45*, 455.

(13) Klauder, J. R.; Skagerstam, B. S. *Coherent States*; World Scientific: Singapore, 1985.

(14) Child, M. S. *Semiclassical mechanics with molecular applications*; Oxford University Press: Oxford, 1991.

(15) Gradsteyn, I. S.; Ryzhik, I. M. *Tables of Integrals, Series and Products*, 5th ed.; Academic Press: New York, 1994.